MOLECULAR AND CELLULAR BIOLOGY, Mar. 1992, p. 962–970
0270-7306/92/030962-09$02.00/0

Vol. 12, No. 3

Identification of *cis*-Acting Intron and Exon Regions in Influenza Virus NS1 mRNA That Inhibit Splicing and Cause the Formation of Aberrantly Sedimenting Presplicing Complexes

MARTIN E. NEMEROFF,[1] ULRIKE UTANS,[2] ANGELA KRÄMER,[2] AND ROBERT M. KRUG[1]*

Department of Molecular Biology and Biochemistry, Center for Advanced Biotechnology and Medicine, Rutgers University, 679 Hoes Lane, Piscataway, New Jersey 08855-1179,[1] and Department of Cell Biology, Biocenter, University of Basel, CH-4056, Basel, Switzerland[2]

Received 23 October 1991/Accepted 10 December 1991

In in vitro splicing reactions, influenza virus NS1 mRNA was not detectably spliced, but nonetheless very efficiently formed ATP-dependent 55S complexes containing the U1, U2, U4, U5, and U6 small nuclear ribonucleoproteins (snRNPs) (C. H. Agris, M. E. Nemeroff, and R. M. Krug, Mol. Cell. Biol. 9:259–267, 1989). We demonstrate that the block in splicing was caused by two regions in NS1 mRNA: (i) a large intron region (not including the branchpoint sequence) and (ii) an 85-nucleotide 3′ exon region near the 3′ end of the exon. After removal of both of these regions, the 5′ and 3′ splice sites and branchpoint of NS1 mRNA functioned efficiently in splicing, indicating that they were not defective. The two inhibitory regions shared one property: splicing inhibition was independent of the identity of the nucleotide sequence in either region. In other respects, however, the two inhibitory regions differed. The inhibitory activity of the intron region was proportional to its length, indicating that the inhibition was probably due to size only. In contrast, the 3′ exon, which was of small size, was a context element; i.e., it functioned only when it was located at a specific position in the 3′ exon of NS1 mRNA. To determine how these intron and exon regions inhibited splicing, we compared the types of splicing complexes formed by intact NS1 mRNA with those formed by spliceable NS1 mRNA lacking the intron and exon regions. Splicing complexes were formed by using purified splicing factors. The most definitive results were obtained under conditions in which only ATP-dependent presplicing 30S complexes were formed with spliceable NS1 mRNA: intact NS1 mRNA still formed ATP-dependent complexes sedimenting at about 55S, even though the protein components needed for the formation of authentic 55S spliceosomes were not present. We postulate that the NS1 mRNA intron and exon regions inhibit splicing by not allowing NS1 mRNA to be folded properly into a substrate for splicing. In fact, the small 85-nucleotide-long 3′ exon region by itself may block proper folding of NS1 mRNA, as the ATP-dependent presplicing complexes formed with NS1 mRNA lacking the intron region also sedimented aberrantly, at approximately 45S rather than 30S. The possible role of the regions in the regulation of NS1 mRNA splicing in vivo is discussed.

During the initial phase of in vitro splicing, pre-mRNA substrates are assembled into large 50S-60S complexes containing five small nuclear ribonucleoproteins (snRNPs), the U1, U2, U4, U5, and U6 snRNPs (4, 6, 9, 12, 26). The U1 and U2 snRNPs bind to the 5′ splice site and intron branchpoint of the pre-mRNA, respectively (5, 24, 34); the U5 snRNP probably binds to the 3′ splice site (7, 25). These large complexes, or spliceosomes, contain the products of the first step in splicing, the 5′ exon and lariat-3′ exon (4, 6, 9, 12, 26).

Influenza virus NS1 mRNA is spliced to form a smaller mRNA, NS2 mRNA. Because both the unspliced (NS1) and spliced (NS2) mRNAs code for proteins, the extent of splicing is regulated in infected cells such that the steady-state level of spliced NS2 mRNA is only about 10% of that of unspliced NS1 mRNA (13, 20, 21, 23). This type of splicing regulation also occurs with retroviruses. In in vitro splicing reactions, NS1 mRNA forms 55S complexes containing the U1, U2, U4, U5, and U6 snRNPs, but little or no catalysis of the first step in splicing occurs (1, 28). The cause of this block in catalysis was not determined, but the available data argued against the involvement of the 5′ and 3′ splice sites and branchpoint of NS1 mRNA in this block. NS1 mRNA contains consensus 5′ and 3′ splice sites, and the 5′ splice site was shown to be functional in an NS1–β-globin chimeric precursor (28). Further, the association of the U1, U2, and U5 snRNPs with the NS1 mRNA in the 55S complexes suggested that these snRNPs bind to the 5′ splice site, 3′ splice site, and branchpoint of NS1 mRNA (1). On the basis of these observations, it was postulated that some other regions in NS1 mRNA blocked the catalysis of splicing.

In this study, we identify two such regions: (i) a large intron region (not including the branchpoint) and (ii) an 85-nucleotide 3′ exon region near the 3′ end of the exon. After removal of these regions, the 5′ and 3′ splice sites and branchpoint of NS1 mRNA function efficiently in splicing. Our results indicate that these two regions block splicing by causing the formation of aberrant presplicing complexes that sediment more rapidly than do authentic presplicing complexes.

MATERIALS AND METHODS

Construction of NS1 mutants. The NS1 deletion mutant Δ153-465 was derived from plasmid pSP64-NS1 (27) by digestion of the full-length NS1 gene (a *Bam*HI fragment) with *Dde*I, followed by religation and cloning into *Bam*HI-cut pSP64, thereby deleting bases 153 to 465. Intron deletions Δ347-469, Δ153-325, Δ246-428, and Δ192-428 and exon

* Corresponding author.

deletions Δ775-829, Δ775-860, and Δ606-694 were generated by in vitro mutagenesis. Construct intron R.C. (reverse complement) was generated by reinserting the NS1 *Dde*I fragment (comprising nucleotides 153 to 465) in the opposite orientation into *Dde*I-cut NS1 deletion mutant D153-465. The 3′ exon R.C. construct was made by first introducing unique EcoRI restriction sites at positions 775 and 860 of the NS1 gene by in vitro mutagenesis. Then, the 775-to-860 *Eco*RI fragment was reinserted in its opposite orientation. To make the NS1 intron replacement clone, a 322-bp *Sca*I-*Ssp*I restriction fragment from plasmid vector pGEM1 was blunt-end ligated into the unique *Cvn*I site of the NS1 Δ153-465 deletion mutant generated by the ligation of the two *Dde*I fragments. The 3′ exon replacement clone, in which 85 nucleotides from the 3′ exon of a human β-globin pre-mRNA (HβΔ6) were substituted for NS1 3′ exon nucleotides 775 to 860, was generated by using the polymerase chain reaction. Chimeric plasmid pSP64-5′NS1/3′GL, generated from plasmids pSP64-NS1 and pSP64-HβΔ6, has been described previously (28). Plasmid pSP64-5′NS1/intron NS1/3′GL was constructed by cutting pSP64-5′NS1/3′GL (28) with *Nsp*HI and ligating the resulting two fragments with a 415-bp *Nsp*HI fragment from the intron of pSP64. This 415-bp *Nsp*HI fragment was generated after introduction of an *Nsp*HI restriction site at position 489 of the NS1 gene in pSP64 by in vitro mutagenesis.

SP6 transcription. In vitro transcripts labeled with ^{32}P at a high specific activity (1×10^7 to 5×10^7 cpm/μg) were synthesized in 50-μl reaction mixtures containing 2 μg of linearized DNA template, 40 mM Tris-HCl (pH 7.4), 6 mM $MgCl_2$, 4 mM spermidine, 10 mM dithiothreitol, 50 U of RNasin, 400 μM ATP, 400 μM CTP, 150 μM GTP, 500 μM m^7GpppG, 50 μM [α-^{32}P]UTP (40 Ci/mmol), and 15 U of SP6 RNA polymerase (Bethesda Research Laboratories) (1). Globin pre-mRNA and NS1 pre-mRNAs with full-length 3′ exons were derived from SP6 plasmids linearized with *Eco*RI (1, 28). NS1 pre-mRNAs with 3′ exons truncated at nucleotide position 715 were derived from SP6 plasmids linearized with *Asu*II. An avian sarcoma virus (ASV) minigene construct (10) was linearized with *Hpa*I at a position 877 nucleotides from the SP6 transcription start site. The labeled transcripts were isolated by electrophoresis on 5% polyacrylamide–8 M urea gels, electroelution, and ethanol precipitation.

In vitro splicing reactions. Splicing reaction mixtures, in a final volume of 50 μl, containing 20 mM *N*-2-hydroxyethylpiperazine-*N*′-2-ethanesulfonic acid (HEPES)-KOH (pH 7.6), 3.2 mM $MgCl_2$, 3% polyethylene glycol, 0.5 mM ATP, 2 mM dithiothreitol, 20 mM creatine phosphate, 4 μg of creatine phosphokinase per ml, 5×10^5 cpm of labeled RNA transcript, and 25 μl of HeLa cell nuclear extract, were incubated at 30°C for 2 and 4 h (1). The nuclear extract was prepared as previously described (8). The reactions were terminated by the addition of 0.2 ml of 2× PK buffer (200 mM Tris-HCl [pH 7.4], 25 mM EDTA, 300 mM NaCl, 2% sodium dodecyl sulfate) and water to 0.4 ml. Pronase was added to 200 μg/ml, and the mixtures were incubated at 37°C for 30 min. Samples were then extracted with phenol-chloroform-isoamyl alcohol (25:24:1) and chloroform-isoamyl alcohol (24:1) and precipitated with ethanol. The precipitates were redissolved in a solution containing 80% formamide, 10 mM piperazine-*N*,*N*′-bis(2-ethanesulfonic acid) (PIPES; pH 6.4), 1 mM EDTA, 0.05% bromophenol blue dye, and 0.05% xylene cyanol and analyzed on polyacrylamide–8 M urea gels. ^{32}P-labeled *Hin*fI-digested pBR322 DNA fragments were used as molecular weight markers. Densitometric scanning of autoradiograms was performed, and the percentage of total RNA spliced was determined after correcting for the sizes of the unspliced and spliced RNA species.

Sucrose gradient analysis of spliceosomes. Splicing reaction mixtures (50 μl) contained 0.4 mM ATP, 10 mM creatine phosphate, 2.5 mM $MgCl_2$, 50 mM KCl, 10% glycerol, 10 mM HEPES-KOH (pH 7.9), 0.05 mM EDTA, 0.25 mM dithiothreitol, 2.6% (vol/vol) polyvinyl alcohol (Sigma type 2), and 10^6 Cerenkov cpm of uniformly labeled pre-mRNA (40 fmol). Where indicated, ATP and creatine phosphate were omitted. The following amounts of partially purified splicing factors (19, 32) were included in the reaction mixture: 4 μl of SF1, 1 μl of SF2, 2 μl of SF3, 2 μl of U2AF, 4 μl of U1/U5 snRNPs, and 2 μl of U2/U4/U6 snRNPs. Where indicated, SF2 was omitted. The purity and characterization of these partially purified splicing factors are described elsewhere (19, 32). The samples were incubated at 30°C for 2 h and then layered onto 5-ml 10 to 30% sucrose density gradients containing 100 mM KCl, 3 mM $MgCl_2$, and 10 mM HEPES-KOH (pH 7.6) (1). Gradients were centrifuged in an SW50.1 rotor at 48,000 rpm at 4°C for 4.5 h, and 0.25-ml fractions were collected from the bottom of the centrifuge tube. A profile of the ^{32}P-labeled RNA of each gradient was obtained by Cerenkov counting of 50-μl aliquots of each fraction. Yeast ribosomal subunits, run on a parallel gradient, served as sedimentation markers (6).

RESULTS

Sequences in two regions of NS1 mRNA are responsible for the inhibition of splicing in vitro. Our initial strategy for identifying the sequence(s) in NS1 mRNA that block its splicing in vitro was based on our previous studies using NS1–β-globin chimerase (28). A chimera containing the β-globin 5′ exon and 5′ splice site joined to NS1 sequences starting 23 nucleotides downstream from the NS1 5′ splice site was inactive in splicing, indicating that the sequence(s) that block splicing could be anywhere in the intron and/or 3′ exon of NS1 mRNA. In contrast, a chimera containing the NS1 5′ exon and 5′ splice site joined to the intron and 3′ exon of β-globin pre-mRNA (transcribed from plasmid pSP64-5′NS1/3′GL) spliced very efficiently (Fig. 1, lane 1): about 50% of the precursor was spliced. Consequently, by inserting intron and/or 3′ exon sequences from NS1 mRNA into the latter chimera, we should be able to determine which of these sequences inhibit splicing. We first inserted 415 nucleotides of the NS1 intron into the intron of the chimera. This caused a strong inhibition of splicing (Fig. 1, lane 2): only about 5% of the precursor was spliced.

If intron sequences were solely responsible for the inhibition of the splicing of NS1 mRNA, then removal of these sequences from NS1 mRNA itself should make it an efficient substrate for splicing. Deletion of 312 nucleotides of the intron did activate splicing of NS1 mRNA (Fig. 2A, lane 3), but only about 10% of the NS1 mRNA precursor was spliced to form NS2 mRNA. Because of the necessity of minimum intron length for splicing (33), a larger intron deletion was not made. This result suggested that there was a second region of NS1 mRNA that contributed to the inhibition of splicing. To determine whether this region was in the 3′ exon, the NS1 transcript lacking 312 nucleotides of the intron was truncated by removal of the 3′-terminal 175-nucleotide exon sequences plus 26 plasmid nucleotides. The resulting transcript was spliced much more efficiently: 48% of the precursor NS1 mRNA was spliced (Fig. 2A, lane 4).

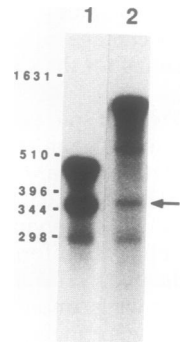

FIG. 1. Inhibition of the splicing of an NS1-globin chimeric pre-mRNA by NS1 intron sequences. pSP64-5'NS1/3'GL and pSP64-5'NS1/intron NS1/3'GL each linearized with *Eco*RI were transcribed with SP6 RNA polymerase. The 5'NS1/3'GL (lane 1) and 5'NS1/intron NS1/3'GL (lane 2) transcripts were incubated with HeLa nuclear extract (50% [vol/vol]) for 2 h at 30°C in the presence of ATP, creatine phosphate, and creatine phosphokinase. The RNA samples were analyzed by denaturing gel electrophoresis on a 7% polyacrylamide gel. The arrow indicates the position of the spliced RNA species. The positions of the splicing intermediates are not denoted. Here and in Fig. 2 to 5, sizes (in nucleotides) of the DNA markers are shown at the left.

However, removal of these 3' exon sequences by themselves, without removal of the intron sequences, did not lead to any detectable splicing (Fig. 2A, lane 2).

The identity of the spliced product was verified by reverse transcription and DNA sequence analysis. The splice sites used in vitro were the same as those used in infected cells (data not shown) (21, 22). In addition, the branchpoint residue used was determined by primer extension of the 3' exon-intron lariat. The branchpoint was localized to an A residue 20 nucleotides upstream from the 3' splice site (data not shown). This is the same branchpoint that was previously identified in the extremely small amount of lariat generated from intact NS1 mRNA in vitro (28). Consequently, the 5' and 3' splice site and branchpoint sequences of NS1 mRNA are functional in splicing but only after removal of the indicated intron and 3' exon sequences.

Localization and characterization of the two inhibitory regions. To localize the inhibitory regions within the intron and 3' exon, various smaller deletions were made. Because efficient in vitro splicing of NS1 mRNA required removal of both intron and 3' exon sequences, all 3' exon deletion mutants tested also had a truncated 3' exon. Splicing reactions were carried out for 2 and 4 h at 30°C; the relative amount of splicing obtained with the various deletions was the same at both time points (data not shown).

The only intron deletion that yielded efficient splicing (of about 50%) was the original 312-nucleotide-long deletion (Fig. 3). Removal of either the 5' portion (Δ153-325) or 3' portion (Δ347-469) of these 312 nucleotides led to barely detectable levels of splicing. As the size of the intron deletion was increased, the efficiency of splicing increased from 5% (Δ246-428) (Fig. 3B, lane 2) to 26% (Δ172-428) to 48% (Δ153-465) (lane 3). Indeed, the efficiency of splicing was directly proportional to the size of the intron deletion in the 172- to 312-nucleotide-long range (Fig. 3C), indicating that the inhibition by the intron sequence was most likely due solely to the size of this sequence. The inhibition was not sequence specific. When the 312-nucleotide-long intron sequence was reinserted in the opposite orientation, splicing was inhibited as efficiently as when this sequence was in its normal orientation (Fig. 4B; compare lanes 1 and 2). In addition, when the NS1 intron sequence was replaced by a random sequence of the same size, splicing was inhibited to the same extent (lane 3).

In contrast to the intron deletions, the exon deletions identified a discrete inhibitory region (Fig. 5). In the absence of a 3' exon deletion, splicing efficiency was only 11%. The first 3' exon deletions tested were shorter 3'-terminal truncations. Removal of only 61 3'-terminal exon nucleotides, plus 26 plasmid nucleotides (mutant truncated at NS1 nucleotide 829, Δ829), did not increase splicing efficiency. This finding indicated that this sequence, including the 26 plasmid nucleotides, did not contribute to the inhibition of splicing.

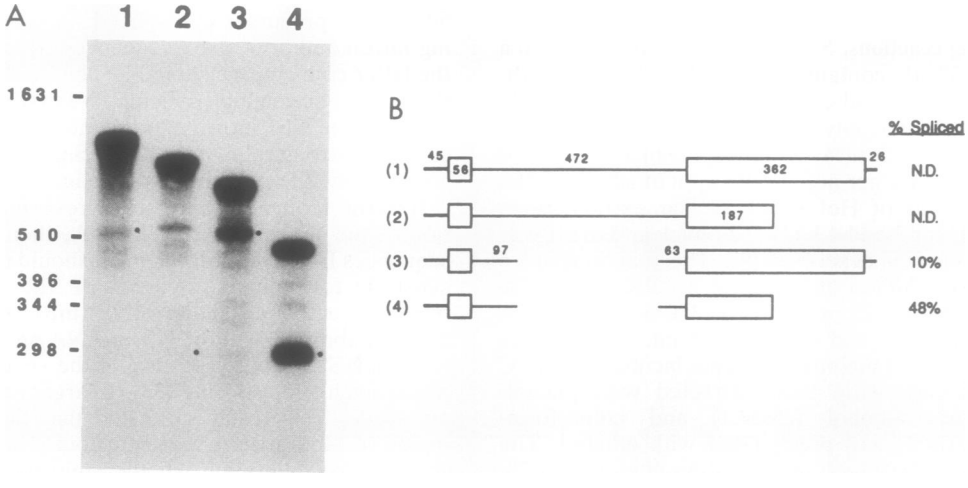

FIG. 2. Identification of NS1 inhibitory regions. (A) NS1 deletion mutants depicted in panel B were subjected to in vitro splicing analysis as described in the legend to Fig. 1. Lanes: 1, wild-type NS1; 2, Δ3' exon; 3, Δintron; 4, Δ3' exon/Δintron. The expected positions of the spliced RNAs are indicated by the black dots. (B) Schematic representation of NS1 deletion mutants. Open boxes represent the two exons, the line between the boxes represents the intron, and the thick lines to the left and right of the boxes represent plasmid sequences. The splicing efficiency of each pre-mRNA is indicated as a percentage of the total RNA spliced (see Materials and Methods).

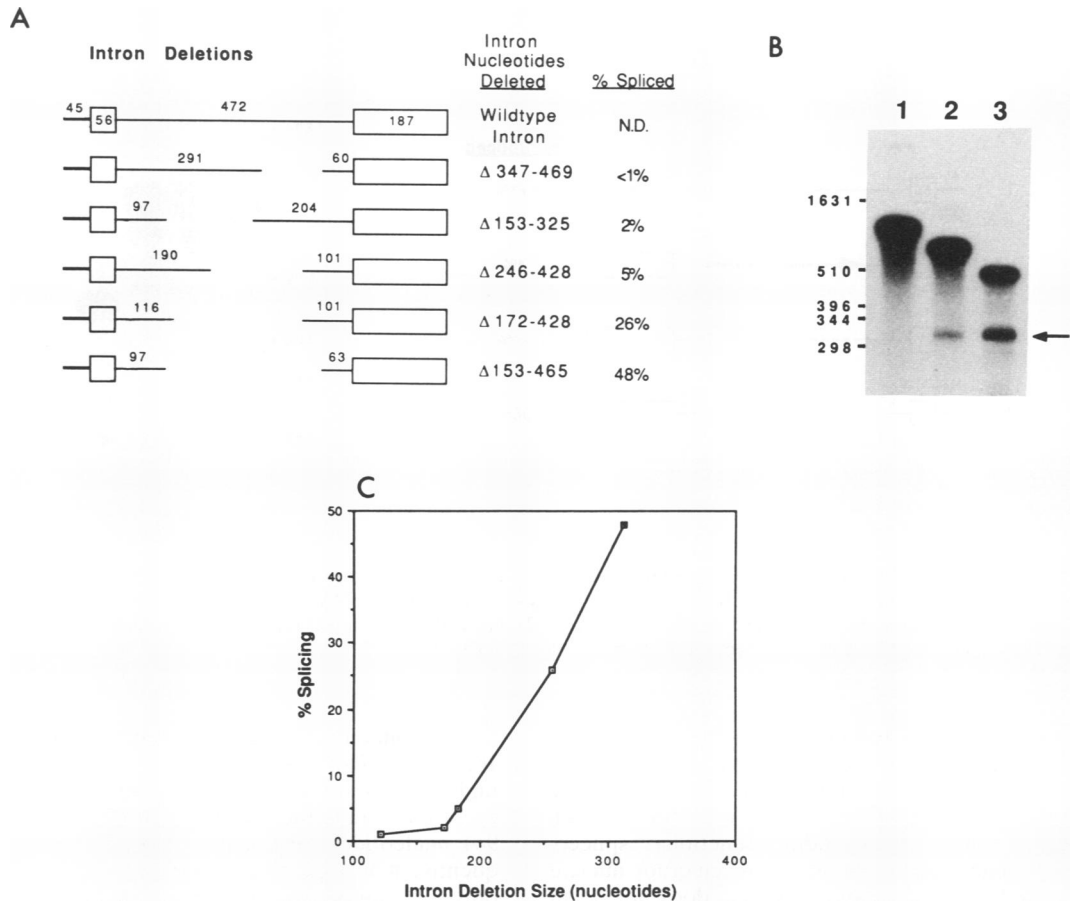

FIG. 3. Localization of the intron inhibitory region. (A) Schematic representation of intron deletions. Deleted introns are represented by gaps. All intron deletions shown have truncated 3′ exons (see Fig. 1). (B) In vitro splicing analysis of representative intron mutant pre-mRNAs, carried out as described in the legend to Fig. 1. Lanes: 1, wild-type intron; 2, Δ246-428; 3, Δ153-465. The arrow indicates the position of the spliced product. (C) Relationship between the size of the intron deletion and the efficiency of splicing.

In contrast, removal of 115 3′-terminal exon nucleotides (mutant truncated at NS1 nucleotide 775) increased splicing efficiency to 48% (Fig. 5B, lane 1), the same efficiency observed with the larger truncation at NS1 nucleotide 715. These results suggested that the inhibitory region was located between nucleotides 775 and 829. Indeed, deletion of the region between 775 and 829 activated splicing to more than 40%. A larger deletion with the same 5′ endpoint (Δ775-860) resulted in slightly higher splicing efficiency, 44% (lane 2). A deletion of the same size at another position in the 3′ exon (Δ606-694) had essentially no effect on splicing efficiency (lane 3), as was also the case for the 87-nucleotide-long 3′-terminal deletion. These results indicated that the inhibition caused by the 775-to-860 region was not simply due to the small (85 nucleotide) increase in the size of the 3′ exon caused by the presence of this region and that the inhibitory sequence was position specific.

The 775-to-860 sequence did not inhibit the splicing of NS1 mRNA when it was moved to the 5′ exon, and this sequence also did not inhibit the splicing of a different precursor, β-globin pre-mRNA, when inserted into the 3′ exon of this precursor at a position comparable to its position in NS1 mRNA (data not shown). To determine whether a specific sequence in the 775-to-860 region was required for inhibitory activity, the sequence was reinserted in its opposite orientation or was replaced by a random sequence of the same size (from the β-globin 3′ exon) (Fig. 6). In both cases, the inhibition was comparable to that obtained with the original 775-to-860 sequence. These results indicated that the 775-to-860 region most likely functioned as a context element, i.e., a position-specific, but not sequence-specific, element that inhibited the splicing of NS1 mRNA but not of other pre-mRNAs.

Effect of the splicing inhibitory regions on the formation of splicing complexes. It was shown previously that despite the almost total absence of splicing intermediates in the in vitro reaction, intact NS1 mRNA efficiently formed ATP-dependent 55S complexes containing the U1, U2, U4, U5, and U6 snRNPs (1). If these 55S complexes represented authentic spliceosome species that were, however, blocked in the subsequent catalysis of splicing, then intact NS1 mRNA and spliceable NS1 mRNA lacking the inhibitory exon and intron sequences should form 55S complexes with similar, if not identical, efficiencies. On the other hand, if these 55S complexes represented aberrant species of splicing complexes, then there would be qualitative or quantitative differences in the types of complexes formed by intact and spliceable NS1 mRNA. For these experiments, it was essential to use conditions under which the dissociation of spliceosomes formed with spliceable pre-mRNAs was mini-

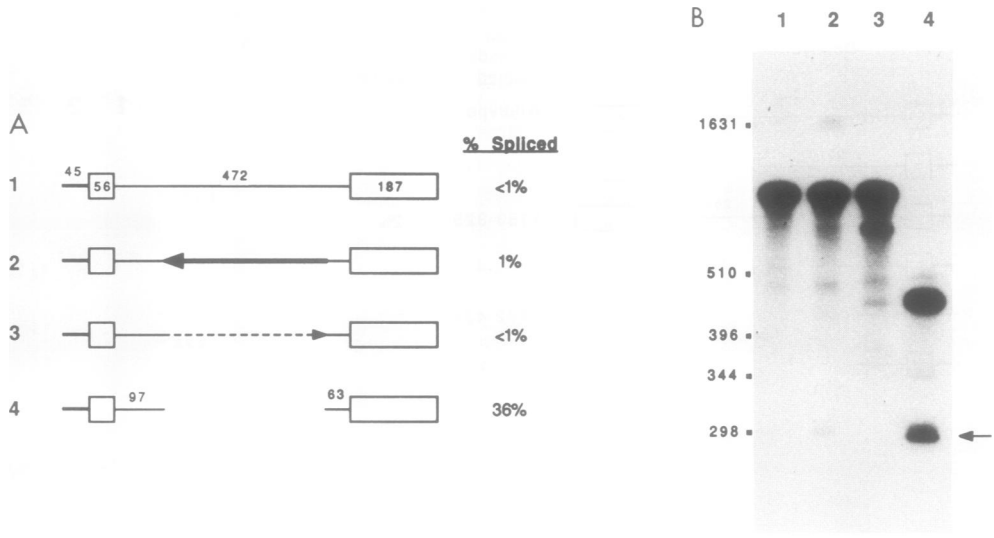

FIG. 4. Characterization of the intron inhibitory region. (A) Schematic representation of NS1 intron constructs. All intron constructs shown have truncated 3′ exons (see Fig. 1). (B) In vitro splicing analysis of the pre-mRNAs containing the various intron constructs, carried out as described in the legend to Fig. 1. Lanes: 1, wild-type intron; 2, intron R.C.; 3, intron replacement; 4, Δ153-465. The arrow indicates the position of the expected spliced product generated from all four precursors.

mized. We used the partially purified splicing factors SF1, SF2 (probably unrelated to the alternative splicing factor SF2/ASF [11, 17]), and SF3, supplemented with U2AF and the U1, U2, U4, U5, and U6 snRNPs. Under these conditions, splicing complexes, including functional spliceosomes, form, though not as efficiently as when crude nuclear extracts are used (32). Catalysis, however, does not occur unless another splicing factor, SF4, is added. In the presence of the full complement of the partially purified splicing factors, globin pre-mRNA and spliceable NS1 mRNA (lacking the inhibitory intron and 3′ exon inhibitory regions) were spliced with similar, albeit relatively low, efficiencies (data not shown). Others have used sucrose density gradients and/or nondenaturing gels to analyze splicing complexes (6, 10, 16, 26). However, we were unable to devise conditions under which several of the splicing complexes, particularly those containing the intact NS1 mRNA transcript, which is 964 nucleotides long, entered nondenaturing gels. Consequently, it was possible to analyze the splicing complexes only by using sucrose density gradients.

Intact NS1 mRNA and spliceable NS1 mRNA lacking the inhibitory intron and exon sequences were each incubated with the partially purified splicing factors (minus SF4) for 2 h at 30°C, and the reaction mixtures were analyzed on sucrose density gradients (Fig. 7). With use of these purified splicing factors, spliceable NS1 mRNA formed 55S spliceo-

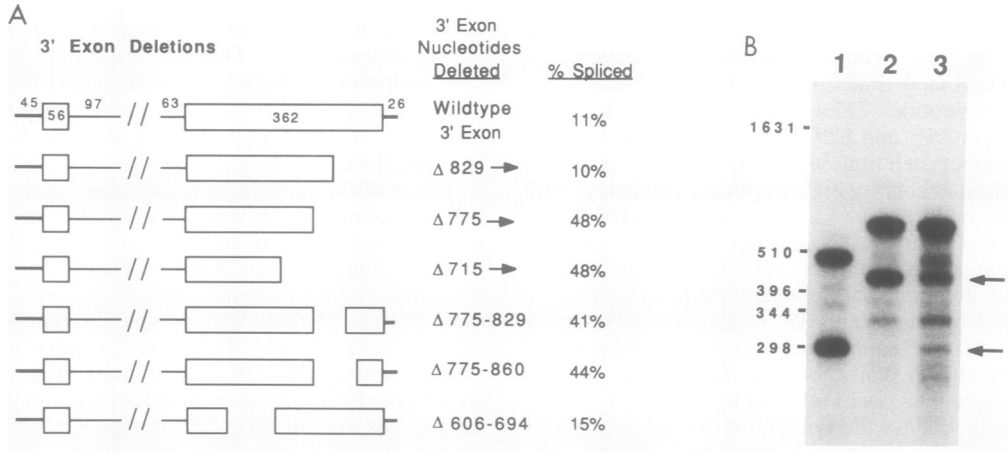

FIG. 5. Localization of the 3′ exon inhibitory region. (A) Schematic representation of 3′ exon deletions. Shortened boxes represent 3′ exons truncated by linearization of plasmid pSP64-NS1 with specific restriction enzymes. Gaps between boxes in the 3′ exon represent internal deletions. The nucleotide positions of these deletions in the NS1 gene are indicated after the Δ symbol (note that nucleotide 1 of the NS1 gene starts at the beginning of the 56-nucleotide 5′ exon). The diagonal lines present in the intron represent an internal deletion (312 nucleotides) of the intron. (B) In vitro splicing analysis of representative 3′ exon mutant pre-mRNAs, carried out as described in the legend to Fig. 1. Lanes: 1, Δ715; 2, Δ775-860; 3, Δ606-694. Arrows indicate the positions of the spliced products (bottom arrow for lane 1 and top arrow for lanes 2 and 3).

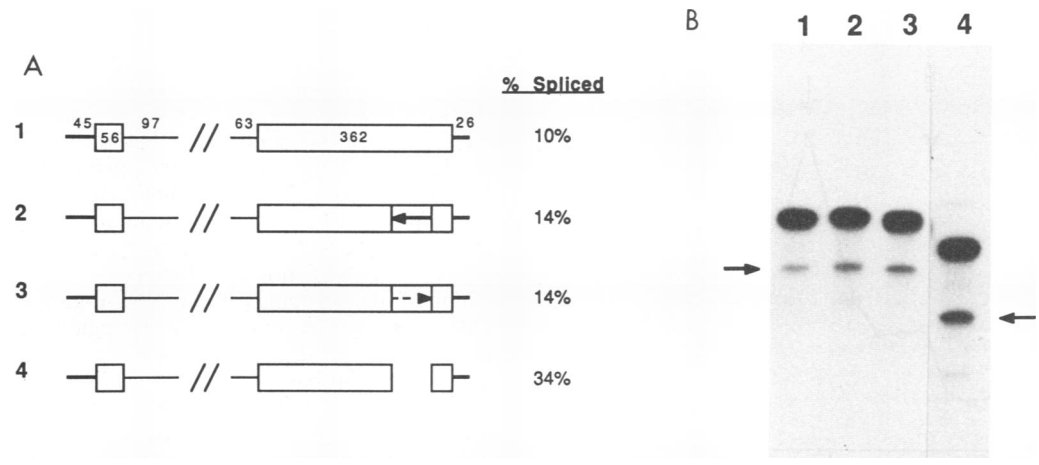

FIG. 6. Characterization of the 3′ exon inhibitory region. (A) Schematic representation of 3′ exon constructs. (B) In vitro splicing analysis of the pre-mRNAs containing the various 3′ exon constructs, carried out as described in the legend to Fig. 1. Lanes: 1, full-length 3′ exon; 2, Δ775-860; 3, Δ775-860 R.C.; 4, 3′ exon replacement. Arrows indicate the positions of the spliced products (arrow on the left for lanes 1 through 3 and arrow on the right for lane 4).

somes approximately as efficiently as did other spliceable pre-mRNAs (32): about 10 to 15% of the input spliceable NS1 mRNA was in 55S complexes (Fig. 7A). These 55S complexes most likely correspond to spliceosomes because they required ATP for their formation and contained splicing intermediates when SF4 was included in the reaction mixture (data not shown). Most (about 60%) of the input spliceable NS1 mRNA was in 30S complexes, which most likely corresponded to the ATP-dependent 30S presplicing complexes described by others (9, 16) (see below). In contrast to spliceable NS1 mRNA, intact NS1 mRNA efficiently formed 55S complexes (Fig. 7B). As shown previously (1), the formation of these 55S complexes was ATP and 3′ splice site dependent. About 60% of input intact NS1 mRNA was in 55S complexes. Little or no 30S complexes were formed. Consequently, the inhibitory intron and exon regions in NS1 mRNA resulted both in an increase in the amount of complexes sedimenting at 55S and in the virtual elimination of 30S complexes.

These results suggested that the 55S complexes formed with intact NS1 mRNA were aberrant complexes rather than authentic spliceosomes that were blocked in subsequent catalysis. To determine whether these aberrant complexes formed during or after the formation of 30S presplicing complexes, we carried out splicing reactions in the absence of splicing factor SF2, conditions under which the formation of presplicing complexes, but not spliceosomes, occurs (18, 19). As expected, spliceable NS1 mRNA lacking the intron and exon sequences formed only ATP-dependent 30S presplicing complexes (Fig. 8C). In contrast, intact NS1 mRNA did not form 30S complexes (Fig. 8A). Rather, it formed ATP-dependent complexes sedimenting at 55S, similar to the sedimentation value of the complexes that were generated in the presence of SF2 (conditions under which 55S spliceosomes form). The large S value of these splicing complexes was not due to the size of intact NS1 mRNA because a precursor RNA of approximately the same size as intact NS1 mRNA, an 877-nucleotide retrovirus pre-RNA that was spliceable in vitro (10), formed only 30S presplicing complexes (Fig. 8D). Some variation in the sedimentation values of the pre-splicing complexes formed with intact NS1 mRNA was observed depending on the amounts of the SF1, SF3, U2AF, and snRNPs added to the reaction mixtures. Under all conditions tested, however, the presplicing complexes formed with spliceable NS1 mRNA sedimented at 30S. We can conclude that intact NS1 mRNA formed aberrant presplicing complexes which were incapable of being converted to functional 55S spliceosomes, even though all five snRNPs eventually become associated with the NS1 mRNA in these complexes (1). To determine whether the 3′ exon inhibitory sequence contributed to the aberrant sedimentation value of the presplicing complexes, NS1 mRNA lacking the inhibitory intron sequence was used. The majority of the ATP-dependent presplicing complexes formed with this RNA sedimented at about 45S rather than 30S (Fig. 8B), indicating that the 3′ exon by itself caused the formation of aberrantly sedimenting complexes.

DISCUSSION

In in vitro splicing reactions, influenza virus NS1 mRNA forms 55S complexes containing the U1, U2, U4, U5, and U6 snRNPs, but little or no catalysis of the first step in splicing occurs (1). We show here that when certain intron and 3′ exon regions are removed, the block in splicing is alleviated, and the 5′ and 3′ splice sites and branchpoint of NS1 mRNA function efficiently. Consequently, the 5′ and 3′ splice sites and branchpoint sequence of NS1 mRNA are not defective. This explains why all previous attempts to activate splicing of NS1 mRNA by changing its 5′ and 3′ splice sites and branchpoint sequence in the presence of the inhibitory intron and 3′ exon elements were unsuccessful (28). For example, changing the branchpoint sequence to UACUAAC, which is complementary to the sequence in U2 snRNA that apparently base pairs with the branchpoint sequence (25), had no effect (25a).

Both the intron and 3′ exon regions had to be removed to achieve optimum splicing efficiency. Removal of the 3′ exon region by itself did not lead to any detectable splicing, whereas removal of the intron region by itself resulted in a low level of splicing, about one-fifth the optimum splicing. These two inhibitory regions shared one property: the splicing inhibition was independent of the identity of the nucleotide sequence in either region. Thus, splicing was also

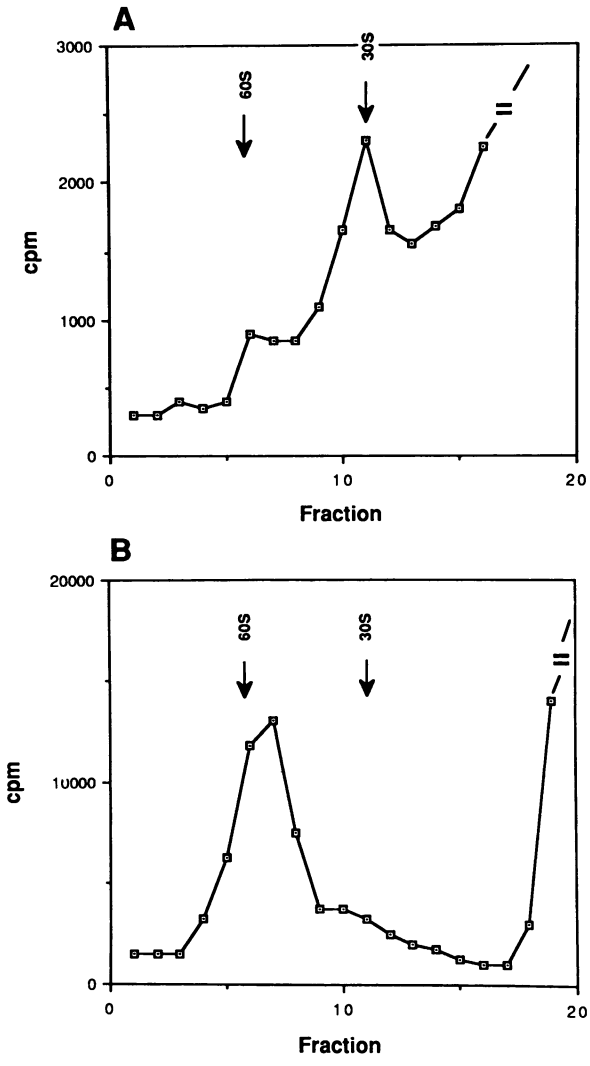

FIG. 7. Evidence that splicing inhibitory regions enhance the formation of 55S complexes. Full-length NS1 mRNA and Δ3′ exon/Δintron (40 fmol of each pre-mRNA) were incubated for 2 h at 30°C with partially purified splicing factors SF1 (4 μl), SF2 (1 μl), SF3 (2 μl), U2AF (2 μl), U1/U5 snRNPs (4 μl), and U2/U4/U6 snRNPs (2 μl) in the presence of both ATP and creatine phosphate, and the reaction mixtures were analyzed on 10 to 30% sucrose gradients. The positions of the 30S and 60S ribosomal markers are shown. (A) Spliceable NS1 mRNA; (B) intact NS1 mRNA. Broken lines at the end of each gradient profile indicate that counts per minute of subsequent fractions was higher than the scale shown.

inhibited when either the intron or 3′ exon region was inserted in the opposite orientation at the same position in NS1 mRNA or when a random sequence was substituted for the authentic NS1 intron or 3′ exon sequence. In other respects, however, the two inhibitory regions differed. The intron inhibitory region was large, comprising at least 312 of the total 472 nucleotides in the NS1 mRNA intron. In NS1 transcripts lacking the inhibitory 3′ exon region, the efficiency of splicing was proportional to the size of the intron deletion, indicating that the inhibition was most likely caused largely, if not totally, by the size of the intron. In contrast, the inhibitory 3′ exon region was discrete and small and mapped to a specific position, between nucleotides positions 775 and 860 in the NS1 mRNA sequence. Other similar-size sequences in the 3′ exon (nucleotide positions 606 to 694 and nucleotide positions 829 to 891) did not inhibit splicing. This finding indicated that the inhibition was not due to the small increase in the size of the 3′ exon caused by the 775-to-860 sequence and that the inhibitory sequence needed to be located at a specific position in the NS1 mRNA 3′ exon. Insertion of the 775-to-860 sequence into the 3′ exon of another pre-mRNA did not inhibit splicing, suggesting that this sequence functions at its normal position only in the 3′ exon of NS1 mRNA. In contrast, the intron region inhibited the splicing of an NS1–β-globin chimeric pre-mRNA, suggesting that the intron region would also inhibit the splicing of other pre-mRNAs. In summary, the intron region most probably inhibits the in vitro splicing of many pre-mRNAs, including NS1 mRNA, primarily if not totally because of its large size, whereas the 3′ exon region, which is of small size, most likely functions only when it is located at a specific position in the 3′ exon of NS1 mRNA.

Insight into the mechanism by which the intron and 3′ exon regions inhibit splicing was obtained from an analysis of the formation of spliceosomes and presplicing complexes. Spliceosomes, which sediment at 55S to 60S and contain the U1, U2, U4, U5, and U6 snRNPs and numerous proteins, have two basic functions: (i) to fold a pre-mRNA into a substrate for splicing, i.e., properly align the splice sites and branchpoint sequence, and (ii) to catalyze the splicing reaction. As shown previously, intact NS1 mRNA forms ATP-dependent 55S complexes containing the U1, U2, U4, U5, and U6 snRNPs, but no catalysis occurs. The results presented here suggest an explanation for the lack of catalysis. It should be emphasized that our experiments were carried out with partially purified splicing factors obtained from uninfected cells, so that only host and not influenza viral factors were involved in the formation of splicing complexes. Under splicing conditions in which spliceable NS1 mRNA (lacking the inhibitory intron and 3′ exon regions) formed only ATP-dependent 30S presplicing complexes, intact NS1 mRNA formed ATP-dependent complexes that sedimented at 55S rather than 30S. Thus, intact NS1 mRNA formed complexes sedimenting at 55S whether or not the protein components (i.e., splicing factor SF2) needed for the formation of authentic 55S spliceosomes were present. This result might be consistent with the binding of additional proteins and/or snRNPs to the intron and 3′ exon sequences during the formation of presplicing complexes. However, it would be surprising if such binding were independent of the identity of the sequence in the intron and 3′ exon regions. In addition, UV cross-linking studies did not detect any additional protein species that bound to the intron or 3′ exon region during the formation of 30S presplicing complexes (unpublished experiments). Alternatively, the aberrant sedimentation value of the presplicing complexes could indicate that the splicing machinery was unable to fold intact NS1 mRNA properly because of the secondary structure constraints caused by the intron and by the 3′ exon regions themselves.

In fact, the small 85-nucleotide-long 3′ exon region by itself may block proper folding of NS1 mRNA by the splicing machinery, as the ATP-dependent presplicing complexes formed with NS1 mRNA lacking the intron region also sedimented aberrantly. These presplicing complexes sedimented at about 45S rather than 30S. How might this small 3′ exon region cause such an effect? One hypothesis is that the 775-to-860 region in the 3′ exon acts as a spacer to allow adjacent regions of NS1 mRNA to interact to form a sec-

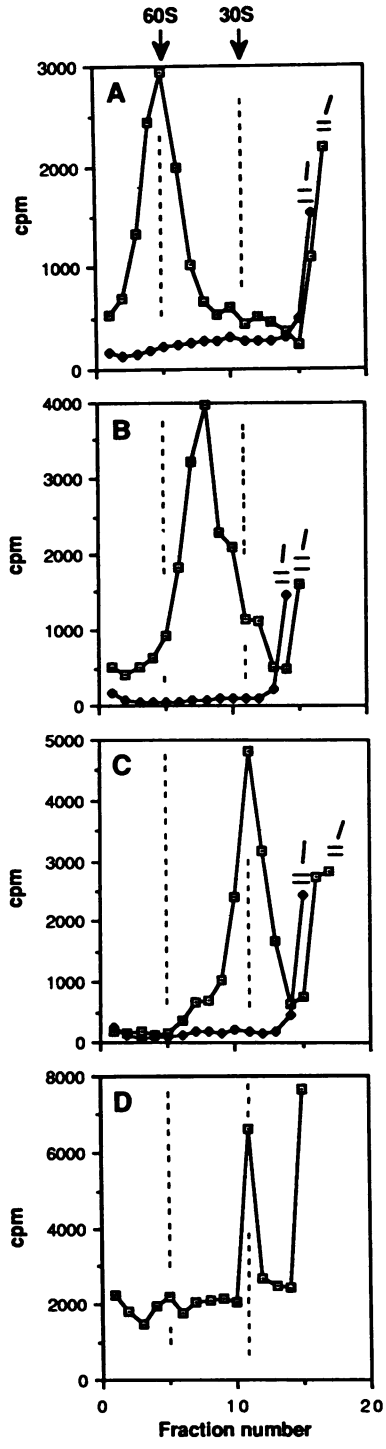

FIG. 8. Aberrant presplicing complex formation by intact NS1 mRNA and by NS1 lacking the intron inhibitory region. Full-length NS1 mRNA, NS1 mRNA lacking the intron inhibitory region (Δintron), spliceable NS1 mRNA (Δ3′ exon/Δintron), and an ASV minigene pre-mRNA (10) were incubated for 2 h at 30°C with partially purified splicing factors SF1 (4 μl), SF3 (2 μl), U2AF (2 μl), U1/U5 snRNPs (4 μl), and U2/U4/U6 snRNPs (2 μl) in the presence (□) or absence (●) of ATP and creatine phosphate, and the reaction mixtures were analyzed on 10 to 30% sucrose gradients. The positions of the 30S and 60S ribosomal markers are shown above panel A and indicated in panels B to D by vertical dashed lines. (A) Full-length NS1 mRNA; (B) NS1 intron mutant (Δintron); (C) spliceable NS1 mRNA (Δ3′ exon/Δintron); (D) ASV pre-mRNA. Broken lines at the end of each gradient profile indicate that the counts per minute in of subsequent fractions was higher than the scale shown.

ondary structure that inhibits proper folding by the splicing machinery, thereby inhibiting splicing. Removal of the 775-to-860 region spacer would then be expected to eliminate the possibility of the interaction of these adjacent sequences and hence the formation of the inhibitory secondary structure. Most of the data are consistent with such a model: the inhibitory sequence most likely needs to be localized in the 775-to-860 region of the 3′ exon, and any sequence in this region is inhibitory to splicing. It is, however, difficult to reconcile one result with this model. The NS1 transcript truncated at nucleotide 829 was inhibited in splicing. In such an NS1 mRNA molecule, the 775-to-829 sequence is at the 3′ end of the molecule and hence could not act as a spacer, though it could conceivably influence the folding of the adjacent 5′ sequences. Clearly, further experiments are needed to determine how this small 3′ exon region causes the formation of aberrantly sedimenting presplicing complexes and the dramatic inhibition of splicing.

In influenza virus-infected cells, the extent of splicing of NS1 mRNA is regulated such that the steady-state amount of spliced NS2 mRNA is about 10% of that of unspliced NS1 mRNA (20, 23). This regulation most likely results from a suppression in the rate of splicing coupled with the efficient transport of unspliced NS1 mRNA from the nucleus (1, 2, 27, 30). Recent experiments have shown that the rate of splicing of NS1 mRNA in infected cells is almost certainly controlled solely by *cis*-acting sequences in NS1 mRNA itself and is independent of *trans*-acting factors (2). Are the intron and/or 3′ exon regions that inhibit splicing in vitro candidates for the *cis*-acting sequences that suppress splicing in vivo? It is likely that the intron region functions only in the in vitro splicing system. Other investigators have found that it is necessary to shorten the intron of pre-mRNAs that are efficiently spliced in vivo in order to obtain efficient splicing in vitro, but these observations have not been clearly documented in the literature. Apparently the in vitro splicing system often does not efficiently splice pre-mRNAs with large introns very well. At least in the case of NS1 mRNA, the long intron apparently did not allow the splicing machinery to fold NS1 mRNA properly during the formation of presplicing complexes. In contrast, the small 3′ exon region might be a candidate for a *cis*-acting sequence that suppresses splicing in vivo. In the presence of the 3′ exon region (and in the absence of the intron region), splicing of NS1 mRNA in vitro occurs to a level of about 10%, which is similar to the extent of splicing in influenza virus-infected cells. Unfortunately, it will be difficult to test this possibility. When NS1 mRNA is expressed with a DNA vector, transport of NS1 mRNA is inefficient and it remains in the nucleus for a relatively long time, where it is extensively spliced (2). Hence, in such a system the rate of transport and not the rate of splicing per se largely determines the extent of splicing. To assess whether the 3′ exon region also acts in vivo, the appropriate 3′ exon deletion will have to be introduced into the genomic RNA of influenza virus by recombinant DNA technology (24). However, because this will eliminate the synthesis of a full-length NS2 protein, it is not clear whether this approach is feasible.

Previous studies have indicated that exon and intron

sequences in other pre-mRNAs influence splicing. For example, exon sequences have been shown to affect the utilization of 5′ and 3′ splice sites in β-globin pre-mRNAs (29). Also, with ASV RNA, intron and 3′ exon sequences have been reported to affect splicing efficiency (3, 14, 15). With ASV RNA, the 3′ exon sequence element was found to enhance splicing efficiency (15), and deletion of this element blocked spliceosome assembly in vitro (10). Splicing of the third intron of P-element pre-mRNA is suppressed in somatic cells of *Drosophila melanogaster*, and this suppression involves the interaction of a 97-kDa protein with 5′ exon sequences (31). Hence, there may be various mechanisms by which exon and intron sequences can affect splicing.

ACKNOWLEDGMENTS

We thank Cheegun Lee for providing HeLa nuclear extract, Tsien-Chen Chang for yeast ribosomal subunit markers, Shu Yun Lee for computer analysis of NS1 RNA folding, and Adrian Goldman for sequence analysis of NS1 mRNA. We also thank A. M. Skalka for providing us with an ASV construct and Helen F. Pirrello for typing the manuscript.

This work was supported by a National Institutes of Health postdoctoral fellowship (1 F32 AI08220-01) to M. E. Nemeroff, by an NIH grant (AI11772, merit award) to R. M. Krug, and by grants from the Kantons of Basel and the Schweizerischer Nationalfonds to A. Krämer.

REFERENCES

1. **Agris, C. H., M. E. Nemeroff, and R. M. Krug.** 1989. A block in mammalian splicing occurring after formation of large complexes containing U1, U2, U4, U5, and U6 small nuclear ribonucleoproteins. Mol. Cell. Biol. **9:**259–267.
2. **Alonso-Caplen, F. V., and R. M. Krug.** 1991. Regulation of the extent of splicing of influenza virus NS1 mRNA: role of the rate of splicing and of the nucleocytoplasmic transport of NS1 mRNA. Mol. Cell. Biol. **11:**1092–1098.
3. **Arrigo, S., and K. Beemon.** 1988. Regulation of Rous sarcoma virus RNA splicing and stability. Mol. Cell. Biol. **8:**4858–4867.
4. **Bindereif, A., and M. R. Green.** 1986. Ribonucleoprotein complex formation during pre-mRNA splicing in vitro. Mol. Cell. Biol. **6:**2582–2592.
5. **Black, L. D., B. Chabot, and J. A. Steitz.** 1985. U2 as well as U1 small nuclear ribonucleoproteins are involved in pre-messenger RNA splicing. Cell **42:**737–750.
6. **Brody, E., and J. Abelson.** 1985. The spliceosome: yeast pre-messenger RNA associates with a 40S complex in a splicing dependent reaction. Science **228:**963–967.
7. **Chabot, B., L. D. Black, D. M. Lemaster, and J. A. Steitz.** 1985. The 3′ splice site of pre-messenger RNA is recognized by a small nuclear ribonucleoprotein. Science **230:**1344–1349.
8. **Dignam, J. D., R. M. Lebovitz, and R. G. Roeder.** 1983. Accurate transcription initiation by RNA polymerase II in a soluble extract from isolated mammalian nuclei. Nucleic Acids Res. **11:**1475–1489.
9. **Frendewey, D., and W. Keller.** 1985. Stepwise assembly of a pre-mRNA splicing complex requires U-snRNPs and specific intron sequences. Cell **42:**355–367.
10. **Fu, X.-D., R. A. Katz, A. M. Skalka, and T. Maniatis.** 1991. The role of branch point and 3′-exon sequences in the control of balanced splicing of avian retrovirus RNA. Genes Dev. **5:**211–220.
11. **Ge, H., and J. L. Manley.** 1990. A protein factor, ASF, controls cell-specific alternative splicing of SV40 early pre-mRNA *in vitro*. Cell **62:**25–34.
12. **Grabowski, P. J., S. R. Seiler, and P. A. Sharp.** 1985. A multicomponent complex is involved in the splicing of messenger RNA precursors. Cell **42:**345–353.
13. **Herz, C., E. Stavnezer, R. M. Krug, and T. Gurney, Jr.** 1981. Influenza virus, an RNA virus, synthesizes its messenger RNA in the nucleus of infected cells. Cell **26:**391–400.
14. **Katz, R. A., M. Kotler, and A. M. Skalka.** 1988. *cis*-acting intron mutations that affect the efficiency of avian retroviral RNA splicing: implication for mechanisms of control. J. Virol. **62:**2686–2695.
15. **Katz, R. A., and A. M. Skalka.** 1990. Control of retroviral RNA splicing through maintenance of suboptimal processing signeals. Mol. Cell. Biol. **10:**696–704.
16. **Konarska, M. M., and P. A. Sharp.** 1986. Electrophoretic separation of complexes involved in the splicing of precursors to mRNAs. Cell **46:**845–855.
17. **Krainer, A. R., G. C. Conway, and D. Kozak.** 1990. The essential pre-mRNA splicing factor SF2 influences 5′ splice site selection by activating proximal sites. Cell **62:**35–42.
18. **Krämer, A.** 1988. Presplicing complex formation requires two proteins and U2 snRNP. Genes Dev. **2:**1155–1167.
19. **Krämer, A., and U. Utans.** 1991. Three protein factors (SF1, SF3 and U2AF) function in pre-splicing complex formation in addition to snRNPs. EMBO J. **10:**1503–1509.
20. **Lamb, R. A., P. W. Choppin, R. M. Chanock, and C.-J. Lai.** 1980. Mapping of the two overlapping genes for polypeptides NS1 and NS2 on RNA segment 8 of influenza virus genome. Proc. Natl. Acad. Sci. USA **77:**1857–1861.
21. **Lamb, R. A., and C.-J. Lai.** 1980. Sequence of interrupted and uninterrupted mRNAs and cloned DNA coding for the two overlapping nonstructural proteins of influenza virus. Cell **21:**475–485.
22. **Lamb, R. A., and C.-J. Lai.** 1984. Expression of unspliced NS1 mRNA, spliced NS2 mRNA, and a spliced chimera mRNA from cloned influenza virus NS DNA in an SV40 vector. Virology **135:**139–147.
23. **Lamb, R. A., C.-J. Lai, and P. W. Choppin.** 1981. Sequences of mRNAs derived from genomic RNA segment 7 of influenza virus: colinear and interrupted mRNAs code for overlapping proteins. Proc. Natl. Acad. Sci. USA **78:**4170–4175.
24. **Luytjes, W., M. Krystal, M. Enami, J. D. Parvin, and P. Palese.** 1989. Amplification, expression and packaging of a foreign gene by influenza virus. Cell **59:**1107–1113.
25. **Maniatis, T., and R. Reed.** 1987. The role of small nuclear ribonucleoprotein particles in pre-mRNA splicing. Nature (London) **325:**673–678.

25a. **Nemeroff, M. E., and R. M. Krug.** Unpublished data.

26. **Perkins, K. K., H. M. Furneaux, and J. Hurwitz.** 1986. RNA splicing products formed with isolated fractions from HeLa cells are associated with fast-sedimenting complexes. Proc. Natl. Acad. Sci. USA **83:**887–891.
27. **Pikielny, C. W., and M. Rosbash.** 1985. mRNA splicing efficiency in yeast and the contribution of nonconserved sequences. Cell **41:**119–126.
28. **Plotch, S. J., and R. M. Krug.** 1986. *In vitro* splicing of influenza viral NS1 mRNA and NS1-β-globin chimeras: possible mechanisms for the control of viral mRNA splicing. Proc. Natl. Acad. Sci. USA **83:**5444–5448.
29. **Reed, R., and T. Maniatis.** 1986. A role for exon sequences and splice—site proximity in splice-site selection. Cell **76:**681–690.
30. **Shapiro, G. I., T. Gurney, Jr., and R. M. Krug.** 1987. Influenza virus gene expression: control mechanisms at early and late times of infection and nuclear-cytoplasmic transport of virus specific RNAs. J. Virol. **61:**764–733.
31. **Siebel, C. W., and D. C. Rio.** 1990. Regulated splicing of the Drosophila P transposable element third intron in vitro: somatic repression. Science **248:**1200–1208.
32. **Utans, U., and A. Krämer.** 1990. Splicing factor SF4 is dispensable for the assembly of a functional splicing complex and participates in the subsequent steps of the splicing reaction. EMBO J. **9:**4119–4126.
33. **Wieringa, B., E. Hofer, and C. Weissmann.** 1984. A minimal intron length but no specific internal sequence is required for splicing the large rabbit β-globin intron. Cell **37:**915–925.
34. **Zhuang, Y., and A. M. Weiner.** 1986. A compensatory base change in U1 snRNA suppresses 5′ splice site mutations. Cell **46:**827–835.